Environ. Sci. Technol. **2003**, *37,* 2988−2996

Biosurfactant- and Biodegradation-Enhanced Partitioning of Polycyclic Aromatic Hydrocarbons from Nonaqueous-Phase Liquids

MARTA GARCIA-JUNCO, CESAR GOMEZ-LAHOZ, JOSE-LUIS NIQUI-ARROYO, AND JOSÉ-JULIO ORTEGA-CALVO*

Instituto de Recursos Naturales y Agrobiología, C.S.I.C., Apartado 1052, E-41080-Seville, Spain

A study was conducted on the effect of two different biological factors, microbial surfactants and biodegradation, on the kinetics of partitioning of polycyclic aromatic hydrocarbons (PAHs) from nonaqueous-phase liquids (NAPLs). The effect of rhamnolipid biosurfactants on partitioning into the aqueous phase of naphthalene, fluorene, phenanthrene, and pyrene, initially dissolved in di-2-ethylhexyl phthalate (DEHP) or 2,2,4,4,6,8,8-heptamethylnonane (HMN), was determined in multiple-solute experiments. Biosurfactants at a concentration above the CMC enhanced the partitioning rate of fluorene, phenanthrene, and pyrene but were ineffective with naphthalene. Enhancement of partitioning was also observed in the presence of suspended humic acid−clay complexes, which simulated the solids often present in the subsurface. Biosurfactants sorbed to the complexes modified PAH partitioning between the NAPL and these solids, increasing the fraction of solid-phase PAH. Biodegradation-driven partitioning was estimated in mineralization experiments with phenanthrene initially present in HMN and three representative soil bacterial strains, differing in their potential adherence to the NAPL. In the three cases, the rates of mineralization were very similar and significantly higher than the abiotic rate of partitioning. Our study suggests that in NAPL-polluted sites, partitioning of PAH may be efficiently enhanced by in situ treatments involving the use of biosurfactants and biodegradation.

Introduction

Polycyclic aromatic hydrocarbons (PAHs) are hydrophobic pollutants often introduced into the subsurface as dense nonaqueous-phase liquid (NAPL) mixtures, such as creosote or coal tar, that represent long-term sources of risk (*1*). Pump-and-treat remediation of soils and aquifers polluted with such mixtures is difficult due to the tendency of these compounds to remain in the separate phase. In situ flushing with synthetic surfactant solutions (*2*) and solvent extraction (*3*) have become alternative techniques to increase the efficiency of NAPL recovery. However, factors such as cost, toxicity, and biodegradability of the surfactants and solvents still limit their application. Some of these problems may be circumvented by in situ biotreatment approaches, which provide some advantages in terms of cost, environmental impact, and social acceptance. Of these alternatives, the use of microbial biosurfactants in flushing solutions (*4*) and the bioremediation of NAPL constituents by indigenous or introduced microorganisms (*5*) can be considered the most viable.

Laboratory and field studies have shown that microbially produced surfactants can be successfully used for environmental applications, for example in remediation of pollution by heavy metals (*6*, *7*), petroleum hydrocarbons (*8*), and BTEX compounds (*4*). It is conceivable, therefore, that biosurfactants could efficiently increase partitioning into the aqueous phase of PAHs present in NAPL mixtures. Biosurfactants typically promote the solubilization of hydrophobic chemicals by forming molecular aggregates, called micelles, which contain hydrophobic domains where the chemicals are incorporated. Indeed, biosurfactants can solubilize pure solid PAHs, such as phenanthrene, increasing their bioavailability and rate of biodegradation (*9, 10*), although micelle-bound PAHs are not available per se and have to be transferred from the micelle to the cell to be assimilated (*11*). To our knowledge, there are no studies on the possible mechanisms involved in partitioning of NAPL-dissolved PAH in the presence of biosurfactants.

The biodegradation of PAH present in NAPLs has been found to be severely limited by the slow kinetics of abiotic mass transfer or partitioning of these hydrophobic compounds into the water phase (*12*). Treatments that promote partitioning, such as slurrying, vigorous shaking, and addition of synthetic surfactants, often have a positive effect on biodegradation rates during laboratory-scale bioremediation of NAPL-polluted soils (*13*−*15*). However, experimental studies with pyrene (*16*), phenanthrene (*17*−*19*), naphthalene (*20*), and styrene (*21*) in NAPL/water systems determined that microorganisms often degrade these hydrocarbons at higher rates than predicted by abiotic partitioning into the bulk aqueous phase. The physicochemical and biological processes causing this poor prediction capacity for biodegradation rates remain to be clarified. They may be related to microbial populations growing at the NAPL/water interface or to the production of biosurfactants that promote partitioning (*5*), but there is little evidence available to support one or other mechanism.

This research constitutes an integrated study on the effect of biosurfactants and biodegradation on partitioning of PAH initially dissolved in NAPLs. We employed a biphasic NAPL/water system with two model NAPLs containing PAHs with different octanol/water partitioning (log K_{ow}) coefficients. The kinetics of partitioning into the aqueous phase was determined in the presence of biosurfactant micelles, model soil solids, and PAH-degrading bacteria. Our main objectives were (i) to compare the effects of biosurfactants on partitioning of different PAHs in different NAPLs, (ii) to determine if degrading bacteria promote partitioning, and, if so, (iii) to determine the possible mechanism(s) involved.

Materials and Methods

Chemicals. Naphthalene, fluorene, phenanthrene, pyrene, di-2-ethylhexyl phthalate (DEHP), 2,2,4,4,6,8,8-heptamethylnonane (HMN), and Triton X-100 were purchased from Sigma Chemical Co., Steinheim, Germany. [^{14}C]-Phenanthrene was also obtained from Sigma (8.3 mCi/mmol, radiochemical purity >98%). The physicochemical constants (at 25 °C) of each of the NAPL constituents used, relevant for

* Corresponding author phone: (+34) 95-4624711; fax: (+34) 95-4624002; e-mail: jjortega@irnase.csic.es.

10.1021/es020197q CCC: $25.00
Published on Web 06/05/2003

this study and available in the literature (*18*, *19*, *22*), are solubility in water or S_w (in mg/L), octanol−water partition coefficient or log K_{ow}, Henry's Law constant K_H (in L atm/mol) or log K_H, density (in g/mL), and viscosity (in cP). The values corresponding to each compound are as follows: naphthalene (S_w: 31; log K_{ow}: 3.36; log K_H: −0.37); fluorene (S_w: 1.9; log K_{ow}: 4.18; log K_H: −1.14); phenanthrene (S_w: 1.1; log K_{ow}: 4.57; log K_H: −1.59); pyrene (S_w: 0.13; log K_{ow}: 5.13; log K_H: −2.05); HMN (S_w: 0.278×10^{-3}; log K_{ow}: 10.1; density: 0.793; viscosity at 22 °C: 3.18); DEHP (S_w: 0.34; log K_{ow}: 7.9; density: 0.981; viscosity at 20 °C: 81.4).

Bacteria, Media, and Cultivation. The bacteria used in this study originated from PAH-contaminated soils and were able to grow with phenanthrene as the sole source of carbon and energy. The *Mycobacterium* strain LB307T was isolated by a novel method using Teflon membranes containing sorbed PAHs for the enrichment and recovery of adherent bacteria from soil; *Sphingomonas* sp. LH128 was isolated through the water-enrichment method (*23*). Both strains were kindly provided by D. Springael (Vlaamse Instelling voor Technologisch Onderzoek, Mol, Belgium). Zeta potentials and water contact angles (θ_W) of bacterial cells, which were grown as described below for mineralization experiments, were, respectively, −22.3 mV and 85.7° for strain LB307T, and −22.9 mV and 32.3° for strain LH128 (M. Lahlou, IRNA, personal communication). According to a classification proposed elsewhere (*24*), the *Mycobacterium* strain is highly hydrophobic, with θ_W above 70°, whereas the *Sphingomonas* strain is hydrophilic, with θ_W below 35°. Neither of these two bacteria produced biosurfactants when growing with phenanthrene as the sole source of carbon and energy, as estimated by surface tension measurements of culture supernatants. *Pseudomonas aeruginosa* 19SJ, a bacterium that produces rhamnolipid biosurfactants when growing with phenanthrene or mannitol (*25*), was also used. It was a gift from E. Déziel (Institute Armand-Frappier, Université du Québec, Canada). Two different media were used to grow the strains: a Tris minimal medium (*23*) for strains LH128 and LB307T and SWF medium for strain 19SJ (*25*). The bacteria were routinely maintained in the corresponding mineral salts medium containing 0.2% (w/v) of phenanthrene which was added in crystalline form.

Biosurfactants. The rhamnolipid biosurfactants produced by *P. aeruginosa* 19SJ were purified, following a procedure described previously (*10*), from cultures grown in 2-L Erlenmeyer flasks that contained 1 L of SWF medium and 10 g of mannitol as the sole source of carbon. The concentration of rhamnolipid was estimated as rhamnose equivalents (RE) with a modified orcinol method (*25*). The detection limit of this method was 1 μg/mL. Surface tension of rhamnolipid solutions diluted with SWF medium was determined at 25 °C with a TD1 Lauda ring tensiometer. The critical micelle concentration (CMC) of rhamnolipid, calculated as the lowest concentration not leading to a significant decrease in surface tension, was 50 μg/mL. This is a commonly determined CMC value for the rhamnolipids produced by *P. aeruginosa* in liquid culture, which are composed mainly of L-rhamnosyl-3-hydroxydecanoyl-3-hydroxydecanoate and L-rhamnosyl-L-rhamnosyl-3-hydroxydecanoyl-3-hydroxydecanoate, besides a small proportion of other congeners with variable-length hydrocarbon chains (C10−C18) (*26*).

Clay and Humic Acid−Clay Complexes. Smectite (Swy-2, University Missouri-Columbia, MO, size < 2 μm) and stable associations of this clay and humic acids (from soils neighboring Santa Olalla lagoon − Doñana National Park, Huelva, Spain) were prepared following procedures described previously (*27*). The fractional organic carbon content (f_{oc}) was 0.013, as determined by elemental analysis performed in a LECO CHNS932 elemental analyzer. Purified clay had undetectable levels of f_{oc}.

Partitioning Experiments. Experiments of PAH partitioning from NAPLs were performed at 25 °C in duplicate according to the constant-interfacial area method of Efroymson and Alexander (*17*). Kinetics of partitioning from NAPLs were determined in 250-mL Erlenmeyer flasks containing 100 mL of sterile SWF medium and the desired amounts of suspended solids (clay and humic acid−clay complexes) and/or biosurfactants. An open-ended glass tube (2 cm in diameter, 10 cm long) was placed vertically in each flask to contain the NAPL. Four slots (6 mm long, 2 mm wide) were cut at the base of the tube to allow exchange of aqueous solution between the inside and outside of the cylinder. One milliliter of NAPL (DEHP or HMN) was added to the surface of the aqueous phase inside the tube. Because of its lower density, it remained floating on the surface of the water phase inside the tube. The NAPL contained 1 mg of phenanthrene, for single partitioning experiments, or 1 mg of each model PAH (naphthalene, phenanthrene, fluorene, and pyrene), for multiple partitioning experiments. The flasks were closed with Teflon-lined stoppers and maintained on a rotary shaker operating at 80 rpm. At time intervals, the aqueous solution outside the glass tube was sampled, and the concentration of PAH in aqueous solution was measured by direct injection into a Waters HPLC system (2690 separations module and 474 scanning fluorescence detector. Column: Nova-Pak C_{18} Waters, 3.9 × 150 mm; flow: 1 mL/min; mobile phase: 60% acetonitrile 40% water; excitation wavelengths (in nm): 270 (naphthalene), 248 (phenanthrene), 270 (fluorene), and 270 (pyrene); emission wavelengths (in nm): 323 (naphthalene), 374 (phenanthrene), 323 (fluorene), and 400 (pyrene). In experiments with suspended solids, the amounts of PAH in solution and associated to solids were determined in the supernatant and in the pellet, respectively, of separate samples (2 mL) that were centrifuged at 12 000 × *g* for 2 min. The pellet was extracted with 2 mL methanol during 5 min, and, after centrifugation to remove the solids, the extract was analyzed by HPLC. Preliminary assays confirmed the efficiency of this procedure for the complete extraction of sorbed PAH. The mild shaking conditions and the use of the tube to contain the NAPL prevented the dispersion of the organic phase. Indeed, no increase in turbidity was observed in the aqueous phase during partitioning experiments with biosurfactant solutions, indicating that the NAPL−water interfacial area remained constant during the experimental period.

In experiments involving suspended model solids (clay and humic acid−clay complexes), the volumes and exchange areas of the different phases were assumed constant during the process. Previous work from this laboratory (*28*) has shown that the initial steps of sorption of PAH to suspended clay and humic acid−clay complexes, leading to a compound sorbed mainly as a "labile" form, are very fast, taking less than an hour to achieve apparent equilibration. Therefore, it was also assumed that sorption to these solids was much faster than partitioning from NAPLs into the aqueous solution, and that desorption from solids was not rate limiting relative to phase transfer from the NAPL. Thus, the hypothesis of local equilibrium between the aqueous phase and the solids was used, while the concentration in the aqueous phase was considered directly proportional to the distance to equilibrium with the NAPL

$$\frac{dC^W}{dt} = k'(C^W{}_{eq} - C^W) \quad (1)$$

$$C^W = K_D C^S \quad (2)$$

where C^W is the aqueous concentration of PAH at time t, $C^W{}_{eq}$ is the aqueous concentration that would be in equilibrium with the NAPL, k' is a mass-transfer rate constant,

C^S is the solid concentration of PAH, and K_D is the aqueous/solid partition coefficient.

To compare the results for treatments with and without suspended solids, a PAH effective aqueous phase concentration, C, was defined as the sum of the mass of PAH in the aqueous and the solid phases per unit volume of aqueous phase. In a similar way, the effective aqueous phase equilibrium concentration, C_{eq}, was defined as the value of C that would be in equilibrium with the NAPL. When no solids were present, the values of C and C_{eq} were equal to C^W and C^W_{eq}.

As long as the local equilibrium hypothesis applies, eq 1 can be rewritten as

$$\frac{dC}{dt} = k(C_{eq} - C) \tag{3}$$

If the value of C_{eq} does not change, the integration yields

$$C = C_{eq}(1 - \exp(-kt)) \tag{4}$$

Calculation of C_{eq} and k was performed by fitting this equation to the experimental data by nonlinear regression. For those cases in which there is a significant depletion of the PAH dissolved in the NAPL, the value of C_{eq} will also decrease with time, and this variation, assuming a linear distribution between the PAH concentrations in the NAPL (C^N) and the aqueous phase ($C_{eq} = KC^N$), can be obtained from the mass conservation as

$$\frac{dC^N}{dt} = \frac{1}{K}\frac{dC_{eq}}{dt} = -\frac{V^W}{V^N}\frac{dC}{dt} \tag{5}$$

where V^W and V^N are the phase volumes. In this case, simultaneous integration of eqs 3 and 5 is required to obtain the values of C_{eq} and k. The maximum rates of effective partitioning were obtained by multiplying the initial value of C_{eq} by k. Statistical comparisons were performed with analysis of variance and Scheffé post-hoc tests at $P = 0.05$.

To assess the possible effect of partitioning from the aqueous phase into the headspace on these rates, controls were run in 250-mL Erlenmeyer flasks containing 100 mL of culture medium and different concentrations of dissolved phenanthrene (0.007 to 0.800 μg/mL). The flasks were maintained at 25 °C and 80 rpm and were periodically sampled for direct HPLC analysis of phenanthrene in solution. No significant decreases in aqueous-phase phenanthrene concentrations (15%—in the control with 0.007 μg/mL—or less) were detected within a time period of 7 h, the period in which the maximum rate of partitioning occurred during the experiences with NAPLs. Because no volatilization controls were run for the other PAHs, it is possible that, according to their somewhat higher Henry's Law constants, the actual rates of partitioning of naphthalene and fluorene may have been slightly underestimated. However, because the flasks were closed with Teflon-lined stoppers during the experiences, no significant losses from the system were expected for any of the four PAHs used.

It is also possible that partitioning of rhamnolipids occurred to some extent into the NAPL phase. Because the main objective of our study was to determine partitioning of PAH, no attempt was made during partitioning experiments to measure actual aqueous biosurfactant concentrations. However, taking into account a dimensionless NAPL-aqueous partition coefficient of 0.31, previously reported for *P. aeruginosa* rhamnolipids (*4*), the total concentrations of rhamnolipids used (10 and 100 μg/mL) were not expected to change significantly. The calculated aqueous concentrations at equilibrium were, respectively, 9.97 and 99.7 μg/mL.

Sorption Experiments. Sorption of biosurfactants to humic acid−clay complexes was determined at 25 °C in 14-mL screw-cap tubes completely filled with SWF medium. The tubes contained 50 mg of complexes and the desired concentration of rhamnolipids, which were completely dissolved into the aqueous phase. These suspensions were equilibrated for 3 h on a rotary shaker operating at 150 rpm and then centrifuged at 12 000 × g for 5 min. The aqueous concentration of rhamnolipids at equilibrium was determined in the supernatant as described above, and the sorbed concentration was calculated by difference. No biosurfactant losses were detected in blank tubes without sorbents. Preliminary experiences showed that a complete equilibration was achieved after 3 h.

Mineralization Experiments. Minimal estimates for partitioning rates of phenanthrene in the presence of degrading bacteria were determined in 250-mL biometer flasks (Bellco glass, NJ) containing the bacterial suspension and 1 mL of NAPL that was placed inside the same glass cylinders used in abiotic partitioning experiments. To prepare bacterial inocula for experiments, the bacterial strains were grown in 2-L Erlenmeyer flasks containing 1 L of the medium of choice and 2 g of phenanthrene at 30 °C on a rotary shaker operating at approximately 200 rpm. Cultures in the late exponential phase were passed through a 40-μm-pore glass frit to remove remaining crystals of the hydrocarbon, and then the cells were collected by centrifugation. The bacterial pellets were washed with buffer at least twice and resuspended in an inorganic salts solution adjusted to pH 5.7, and the number of bacteria was determined as colony-forming units by plating serial dilutions of this suspension on tryptic soy agar (*28*). Duplicate 100-mL portions of the bacterial suspension, containing approximately 10^7, 10^5, or 3×10^7 cells/mL, for strains LH128, LB307T, and 19SJ, respectively, were added to the biometer flasks, and each flask received its glass tube. One milliliter of HMN—containing 40 000 to 60 000 dpm of ^{14}C-labeled phenanthrene and sufficient unlabeled substrate to give 1 mg/mL NAPL—was added to the surface of the aqueous phase inside the tube. Significant bacterial growth was only expected for experiments with strain LB307T, considering the cell densities used, the concentration of substrate initially present (10 μg/mL aqueous phase), and that the amount of substrate needed to form one bacterial cell is approximately 1 pg (*5*). The flasks were closed with Teflon-lined stoppers and incubated at 25 °C on a rotary shaker operating at 80 rpm. $^{14}CO_2$ production was measured as radioactivity appearing in the alkali trap of the biometer flasks. The trap contained 1 mL of 0.5 M NaOH. Periodically, the solution was removed from the trap and replaced with fresh alkali. The NaOH solution was mixed with 5 mL of liquid scintillation cocktail (Ready Safe, Beckman Instruments, Fullerton, CA), and the mixture was kept in darkness for about 8 h for dissipation of chemiluminescence. Radioactivity was measured with a liquid scintillation counter (Beckman Instruments, Inc., Fullerton, CA; model LS5000TD). Biodegradation-driven partitioning rates were estimated directly from maximum mineralization rates. They were calculated as the slope of the regression lines drawn with the points belonging to the phase of maximum mineralization (*20*). The calculated rates were compared to the partitioning rates of phenanthrene measured under the same conditions, but without bacteria nor ^{14}C-labeled phenanthrene, in separate partitioning experiments involving measurements by HPLC. No attempt was made to determine abiotic partitioning rates by using the ^{14}C-labeled compound and liquid scintillation counting, according to the low concentrations expected in the aqueous phase and the radiochemical purity of the chemical (> 98%).

Some mineralization experiments were performed in the presence of 0.1% Triton X-100, a known inhibitor of cell adhesion (*20*, *27*). The critical micelle concentration of this nonionic surfactant, as determined at 25 °C with a TD1 Lauda

ring tensiometer (Lauda, Germany), was 0.01%. The abiotic partitioning of phenanthrene from the NAPL in the presence of this surfactant was also measured in separate partitioning experiments. Some phenanthrene partitioning experiments were also performed in parallel to mineralization assays, after killing the bacteria with 0.5 mL of 40% formaldehyde at the beginning of the phase of maximum mineralization. These flasks were prepared like those for mineralization determinations but contained no ^{14}C-labeled phenanthrene. In these cases, the amounts of PAH in solution and associated to bacterial cells were determined by HPLC as already described for partitioning experiments with suspended solids. Effective partitioning rates and C_{eq} were also calculated as indicated above but excluding the initial phase in which no compound was detected in the aqueous phase.

The adherence of bacteria to HMN was tested with a modified assay of microbial adhesion to hydrocarbons (*25*). HMN (0.25 mL) and 1 mL of the cell suspension, prepared as described above for mineralization experiments, were vortexed in a test tube. After 30 min of equilibration, adhesion was estimated from the loss of absorbance at 400 nm as a result of adhesion to the NAPL.

Results

Partitioning of Phenanthrene from NAPLs. The partitioning of phenanthrene from HMN and DEHP into the aqueous phase is shown in Figure 1A. Phenanthrene partitioning from HMN led to higher aqueous concentrations than from DEHP. The maximum rates of phenanthrene mass transfer into the water phase were 2.7 ± 0.1 ng/mL/h and 0.6 ± 0.0 ng/mL/h when the compound was initially present in HMN and DEHP, respectively. Values for C_{eq} were 50.4 ± 0.4 ng/mL for HMN and 4.4 ± 0.3 ng/mL for DEHP.

Partitioning of phenanthrene from HMN into the aqueous phase was not substantially modified by the presence of solids suspended in the aqueous phase (Figure 1B). Sorption to clay and humic acid−clay particles led during the experiments to somewhat lower aqueous concentrations of phenanthrene. Figure 1B shows a good agreement between predicted and experimentally determined phenanthrene concentrations, indicating that the model adequately describes partitioning from a NAPL. Sorption to the organic-free clay particles in such aqueous system was low, although it was measurable. The calculated equilibrium concentrations in the solid phase were 4.1 ± 1.0 and 13.4 ± 1.6 ng/mg for clay and humic acid−clay particles, respectively. The greater capacity of the complexes to sorb phenanthrene was probably attributable to the presence of organic matter in the particles, to which this hydrophobic compound may have associated (*28*).

Effect of Biosurfactants on PAH Partitioning. Since PAHs usually exist in the environment not as individual compounds but as mixtures, multiple partitioning experiments were conducted with naphthalene, fluorene, phenanthrene, and pyrene. The PAHs were dissolved in HMN or DEHP at 1 mg/mL, and their partitioning into the water phase was measured simultaneously in the presence of biosurfactants at concentrations below (10 μg/mL) and above (100 μg/mL) the CMC. Without biosurfactants, partitioning into the water phase had an inverse relationship with the log K_{ow} of the compounds, the aqueous concentrations being higher with naphthalene, lower with fluorene and phenanthrene, and lowest with pyrene (Figure 1C). The partitioning rates and C_{eq} values calculated by nonlinear regression of these results with eq 3 are shown in Table 1. It should be noted that the resulting partitioning rate of phenanthrene was somewhat higher than the obtained in single-solute experiments (Figure 1A). The differences were, however, not statistically significant.

The effect of biosurfactants on partitioning rate and C_{eq} depended strongly on the identity of the PAH and the NAPL

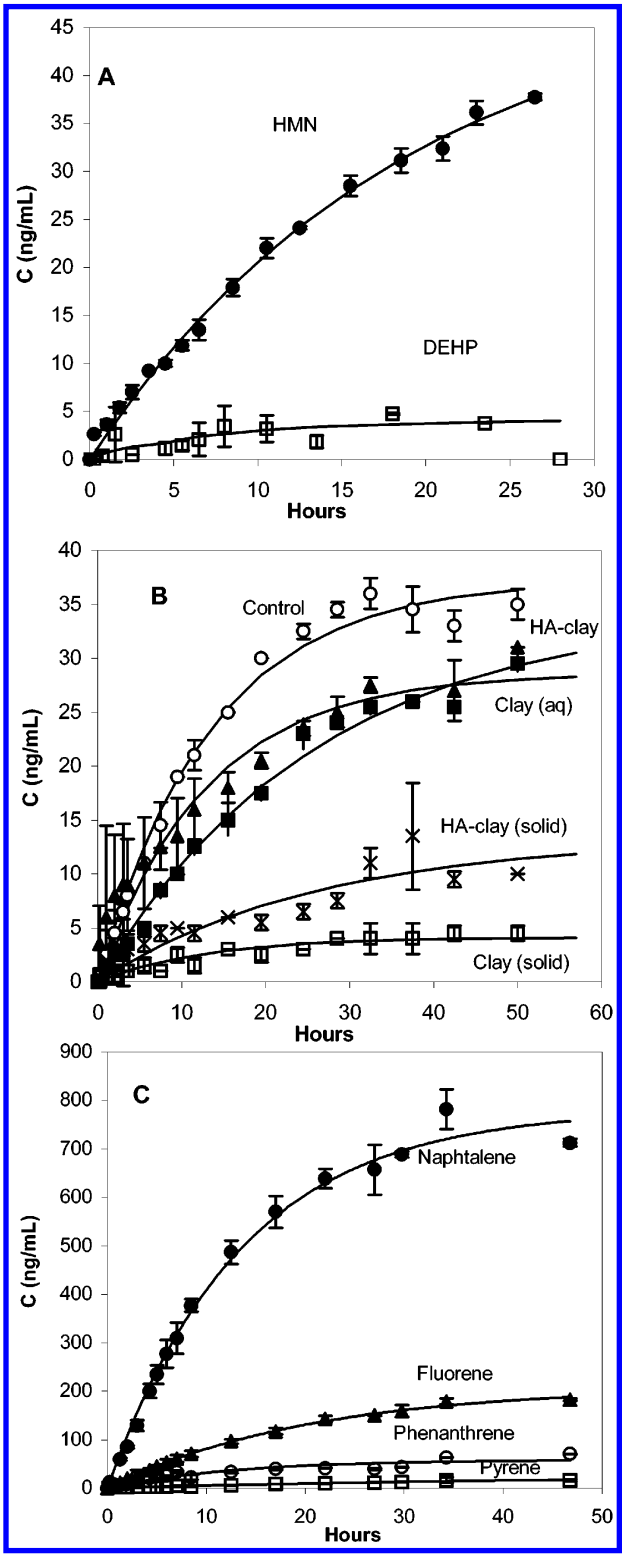

FIGURE 1. (A) Partitioning of phenanthrene from HMN (●) and DEHP (□). (B) Influence of suspended clay and humic acid−clay particles on partitioning of phenanthrene from HMN. Symbols represent phenanthrene concentrations (in ng/mL for all cases) in the aqueous phase without solids (○), with clay (▲), and humic acid−clay complexes (■) and in the solid phase of suspensions containing clay (□) or complexes (×). (C) Multiple partitioning experiment showing partitioning of naphthalene (●), fluorene (▲), phenanthrene (○), and pyrene (□) from HMN. Solid lines represent fits to eq 3. Error bars represent standard deviations of duplicate experiments.

(Table 1). Biosurfactants did not cause statistically significant increases in the rate of partitioning of naphthalene, in either

TABLE 1. Effect of Biosurfactants on Partitioning of PAHs from Nonaqueous-Phase Liquids[a]

PAH	NAPL	biosurfactant (μg/mL)	partitioning rate (ng/mL/h)	C_{eq} (ng/mL)
naphthalene	HMN	0	60.0 ± 4.5A	846.6 ± 15.0A
		10	72.0 ± 10.8A	920.8 ± 15.1A
		100	86.5 ± 5.9A	1415.4 ± 10.0B
	DEHP	0	15.3 ± 5.8A	135.6 ± 10.0A
		10	17.4 ± 11.0A	125.9 ± 3.3A
		100	21.4 ± 1.5A	137.4 ± 2.4A
fluorene	HMN	0	10.3 ± 1.0A	214.5 ± 2.0A
		10	13.2 ± 1.6A	308.2 ± 25.8A
		100	25.0 ± 4.7B	1365.2 ± 98.4B
	DEHP	0	1.4 ± 0.4A	22.2 ± 1.1A
		10	1.5 ± 0.5AB	21.30 ± 2.6A
		100	3.5 ± 0.5B	34.5 ± 2.2B
phenanthrene	HMN	0	4.8 ± 1.4A	59.6 ± 7.8A
		10	9.4 ± 2.5A	96.1 ± 24.7A
		100	27.7 ± 0.1B	636.4 ± 10.0B
	DEHP	0	0.5 ± 0.0A	4.4 ± 0.2A
		10	1.5 ± 0.5A	4.6 ± 0.2B
		100	78.7 ± 18.9B[b]	15.1 ± 1.1C
pyrene	HMN	0	0.5 ± 0.0A[c]	17.8 ± 4.2A[d]
		10	1.6 ± 0.6A[c]	85.1 ± 27.8B[d]
		100	11.6 ± 0.4B[c]	547.4 ± 18.6C[d]

[a] Reported values are means ± one standard deviation. For each PAH and NAPL, values in a column followed by the same capital letter are not significantly different ($P = 0.05$). [b] Due to fast partitioning, the value reported was calculated from the first time point taken after 15 min. [c] Values calculated by linear regression with 10 time points (first 24 h). [d] Maximum experimental values because no equilibrium was achieved within the experimental period.

TABLE 2. Influence of Biosurfactants on Partitioning of PAHs between Heptamethylnonane and Suspensions of Model Subsurface Solids[a]

PAH	solids (mg/mL)	biosurfactants (μg/mL)	partitioning rate (ng/mL/h)	C_{eq} (ng/mL)	eq concn in solids (ng/mg)	K_d[b] (mL/g)
naph.	none	none	60.0 ± 4.5A	846.6 ± 15.0A	NA[c]	NA
	1	none	62.7 ± 13.6A	896.7 ± 124.4AC	42.5 ± 4.3A	50.7 ± 12.7A
	2	none	56.1 ± 7.2A	912.7 ± 105.1AC	26.1 ± 5.4A	30.2 ± 3.0A
	1	10	65.8 ± 2.3A	882.6 ± 25.3AC	53.7 ± 12.9AB	64.7 ± 14.6A
	1	100	113.4 ± 9.7AB	1748.7 ± 247.0B	88.1 ± 7.5B	53.3 ± 3.2A
fluor.	none	none	10.3 ± 1.0A	214.5 ± 2.0A	NA	NA
	1	none	10.9 ± 1.7A	218.8 ± 13.9A	25.4 ± 3.3A	131.1 ± 9.6A
	2	none	8.7 ± 0.5A	246.5 ± 23.5A	20.8 ± 2.6A	101.2 ± 3.4A
	1	10	10.9 ± 0.4A	224.0 ± 10.8A	41.2 ± 7.9A	224.9 ± 39.9B
	1	100	42.4 ± 1.2C	1202.4 ± 270.4B	83.9 ± 11.3B	75.9 ± 7.5A
phen.	none	none	4.8 ± 1.4A	59.6 ± 7.8A	NA	NA
	1	none	5.1 ± 1.5A	60.2 ± 3.1A	12.9 ± 1.4A	271.0 ± 20.2A
	2	none	2.9 ± 0.9A	111.7 ± 39.9A	14.4 ± 4.1A	176.3 ± 17.3AB
	1	10	4.8 ± 0.2A	79.0 ± 3.6A	25.1 ± 4.0AB	464.4 ± 76.9C
	1	100	93.5 ± 1.9C	608.9 ± 15.9B	32.1 ± 4.6B	55.7 ± 6.8B
pyr.	none	none	0.5 ± 0.0A[d]	17.8 ± 4.2A[e]	NA	NA
	1	none	0.7 ± 0.4A[d]	26.6 ± 2.1AB[e]	15.8 ± 1.6A[e]	1574.2 ± 674.7A[e]
	2	none	1.0 ± 0.3A[d]	26.6 ± 0.5AB[e]	10.6 ± 0.3A[e]	329.0 ± 25.0A[e]
	1	10	1.7 ± 0.4A[d]	26.3 ± 2.6AB[e]	16.3 ± 6.6A[e]	1878.4 ± 1379.8A[e]
	1	100	27.4 ± 1.1C[d]	650.4 ± 12.7D[e]	39.6 ± 1.8B[e]	64.7 ± 1.8A[e]

[a] Reported values are means ± one standard deviation. For each PAH, values in a column followed by the same capital letter are not significantly different ($P = 0.05$). Statistical analysis of partitioning rates and C_{eq} were performed together with those shown in Table 1 for HMN. [b] K_d, solids/aqueous phase distribution coefficient. [c] NA, not applicable. [d] Values calculated by linear regression with 10 time points (first 24 h). [e] Maximum experimental values because no equilibrium was achieved within the experimental period.

HMN or DEHP, compared with the control. The rates of partitioning of fluorene, phenanthrene, and pyrene were significantly increased by 100 μg/mL biosurfactants. The increase was highest (more than 20-fold) in the case of pyrene. Statistically significantly higher values of C_{eq} were also determined in the presence of biosurfactants (100 μg/mL) in the four PAHs when they were initially dissolved in HMN. The relative enhancements of partitioning rate and C_{eq} were positively correlated with the hydrophobicity of the compounds. In DEHP, biosurfactants increased C_{eq} of fluorene and phenanthrene, although to a lesser extent than in HMN, and were ineffective with naphthalene. Biosurfactants at a concentration below the CMC (10 μg/mL) caused increases in partitioning rates and C_{eq} values, but the differences were statistically significant only for C_{eq} of pyrene initially present in HMN.

Partitioning experiments were also performed with the four PAHs dissolved in HMN and aqueous suspensions of humic acid−clay complexes, which simulated the suspended solids that are often present in the subsurface. The results of these experiments are shown in Table 2. Without biosurfactants, the four PAHs sorbed significantly to the solids, which led to a total PAH concentration of 96.6 mg/kg in suspensions containing 1 mg/mL solids. The effective partitioning rates (i.e., calculated from the sum of each PAH partitioned into the aqueous phase plus that sorbed to the

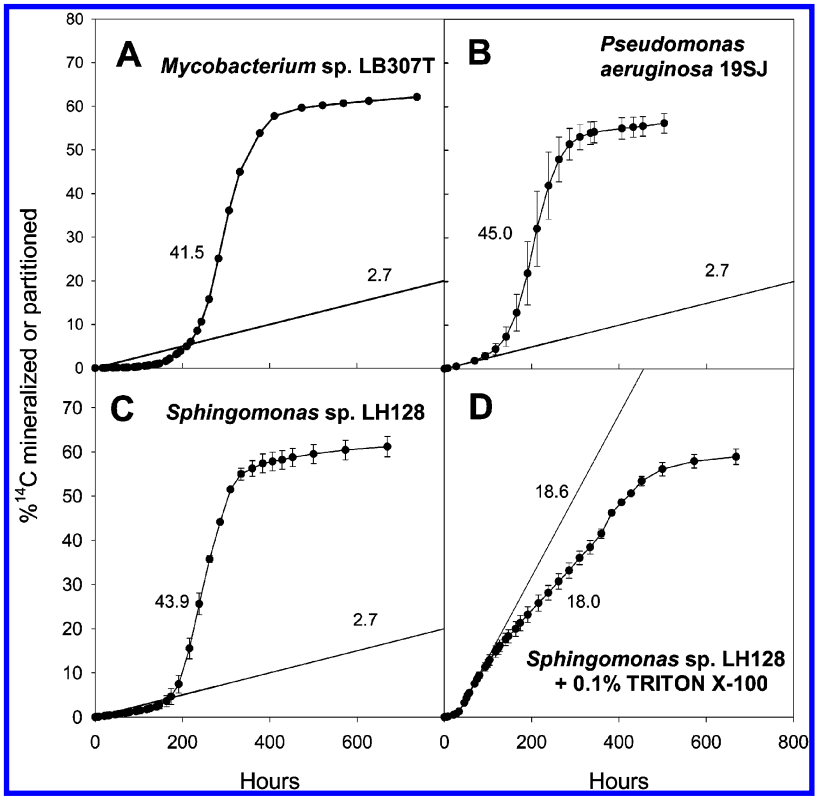

FIGURE 2. Mineralization of phenanthrene initially present in HMN by selected strains of PAH-degrading bacteria. (A) *Mycobacterium* sp. LB307; (B) *Pseudomonas aeruginosa* 19SJ; (C) *Sphingomonas* sp. LH128; (D) *Sphingomonas* sp. LH128 with 0.1% Triton X-100. Solid lines represent biodegradation predicted by maximum abiotic partitioning rate determined in single-solute experiments (Figure 1A). The numbers denote maximum rates (in ng/mL/h) of predicted and experimentally determined biodegradation. Error bars represent standard deviations of duplicate experiments.

solids) of none of the PAHs were significantly affected by doubling the concentration of suspended solids or by a low concentration of biosurfactants (10 μg/mL). However, suspensions of humic acid−clay complexes containing biosurfactants at 100 μg/mL enhanced the effective partitioning rates of the four PAHs tested. At a biosurfactant concentration above the CMC, the resulting partitioning rates were higher in the presence of model solid particles than in their absence (Table 1) for fluorene, phenanthrene, and pyrene. Values for C_{eq} were also statistically higher for pyrene (547.4 and 650.4 ng/mg without and with complexes, respectively).

The values of the solids/water distribution coefficient, K_D, obtained in suspensions with 10 μg/mL biosurfactants were, for fluorene and phenanthrene, also higher than in the absence of rhamnolipids (Table 2). This suggests an enhanced PAH-sorption capacity of the solids induced by sorbed biosurfactants. Sorption of biosurfactants to the solids was determined in separate batch experiments. Suspensions containing humic acid−clay complexes and 30 or 87 μg RE/mL rhamnolipids were equilibrated for 2 h. After centrifugation, the concentrations of biosurfactants remaining in solution were, respectively, 19.35 ± 0.35 μg RE/mL (reflecting a solid-phase rhamnolipid concentration, C_s, of 2.98 ± 0.10 μg RE/mg) and 63.03 ± 2.05 μg RE/mL (C_s = 6.72 ± 0.57 μg RE/mg). However, in partitioning experiments (Table 2) only at a concentration of 100 μg/mL did the biosurfactants cause statistically higher contents of individual PAHs in the suspended solids. This resulted in doubling the final content in total PAH (243.6 mg/kg), compared with the control without biosurfactants. At this concentration of rhamnolipid, the values for K_D were, however, not statistically different or (as in the case of phenanthrene) even lower than without biosurfactants.

Effect of Biodegradation on Phenanthrene Partitioning. To assess the effect of degrading bacterial populations on partitioning of PAH from NAPLs, a set of mineralization experiments was performed with ^{14}C-labeled phenanthrene dissolved in HMN. Minimal estimates for partitioning rates of the ^{14}C-labeled compound were determined as $^{14}CO_2$ appearing in the NaOH traps of biometer flasks. Three different phenanthrene-degrading bacteria were used, i.e., the hydrophobic *Mycobacterium* sp. LB307T, the hydrophilic *Sphingomonas* sp. LH128, and a strain capable of producing rhamnolipid biosurfactants from phenanthrene (*Pseudomonas aeruginosa* 19SJ). However, irrespective of the strain used, the curves for phenanthrene mineralization were S-shaped, exhibiting an initial slow phase that lasted approximately the first 150 h, followed by a rapid phase that ended with a period of slower mineralization (Figure 2A−C). The amount of substrate mineralized at the end of the experimental period was approximately 60%. The maximum rate of mineralization observed during the rapid phase was similar for the three strains (41.5 to 45.0 ng/mL/h) but significantly higher than the partitioning rate measured in the absence of bacteria (2.7 ng/mL/h).

To investigate the mechanism by which bacteria increased the rate of partitioning, the mineralization of phenanthrene by *Sphingomonas* sp. LH128 was measured in the presence of Triton X-100. Despite the hydrophilic character of this strain, a significant fraction (28.94%) of the initial bacterial population showed, in separate adhesion assays, the potential capacity to adhere to the NAPL phase. The other two bacteria showed a somewhat higher capacity of adhesion to HMN (39.00% for *Pseudomonas aeruginosa* 19SJ and 65.54% for *Mycobacterium* sp. LB307T). In the presence of this inhibitor of cell adhesion, the mineralization curve was totally different from that observed without surfactant (Figure 2D). The initial slow phase was shortened to a few hours, and the subsequent maximum rate of mineralization (18.0 ng/mL/h) was not statistically different to the abiotic partitioning rate (18.6 ng/

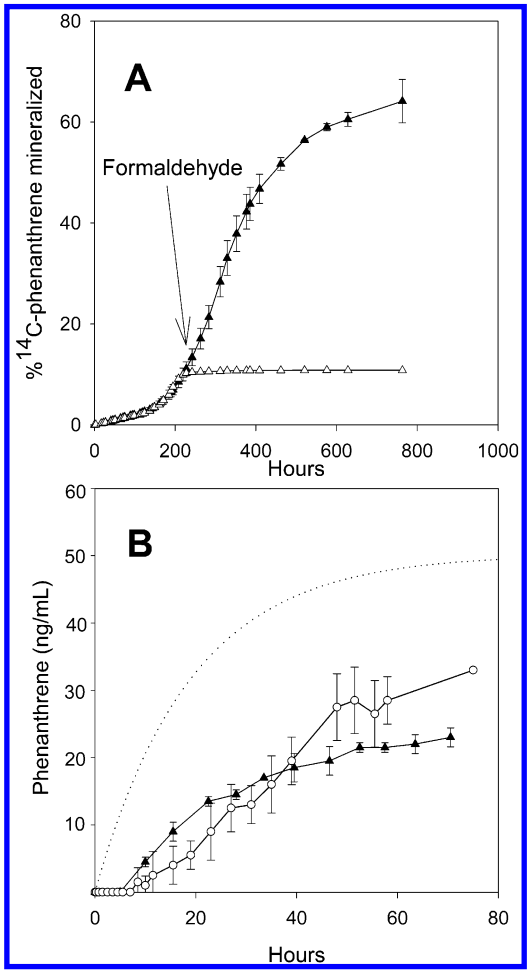

FIGURE 3. Effect of formaldehyde on phenanthrene mineralization and subsequent partitioning of the compound initially present in HMN at 1 mg/mL. (A) Mineralization curve with *Sphingomonas* sp. LH128 showing the point at which the biocide was added to the aqueous phase. Open and filled symbols represent, respectively, flasks with and without formaldehyde addition. (B) Concentrations of phenanthrene appearing in the aqueous phase after killing *Sphingomonas* sp. LH128 (▲) or *Pseudomonas aeruginosa* 19SJ (○) at the beginning of the phase of maximum mineralization. For results with *Sphingomonas* sp. LH128, time zero in (B) relates in (A) to the point where formaldehyde was added (indicated by the arrow). The dotted line represents abiotic partitioning of phenanthrene at 1 mg/mL NAPL as predicted by eq 3. Error bars represent standard deviations of duplicate experiments.

mL/h). Mineralization then proceeded at progressively lower rates, reaching a final amount of substrate mineralized similar to that observed without Triton X-100.

The possible contribution to the observed mineralization rates by partitioning-promoting agents present in the aqueous phase was also investigated. A mineralization-partitioning experiment was conducted with *Sphingomonas* sp. LH128, in which bacteria were killed with formaldehyde at the beginning of the phase of maximum mineralization. The addition of the biocide, at a time point when approximately 10% of the compound had been recovered as $^{14}CO_2$, resulted in the immediate and complete inhibition of $^{14}CO_2$ evolution (Figure 3A). The aqueous concentration of phenanthrene, as measured by HPLC, was at this time below the detection limit (2 ng/mL). The compound appeared in the aqueous phase 10 hours later, as a result of partitioning from the NAPL (Figure 3B). This confirms the compatibility between HPLC and ^{14}C measurements in the experimental system used. Subsequent sorption to suspended bacterial biomass led, at equilibrium, to a small fraction of the compound associated to cells (4.5 ± 0.7 ng/mL). The measured rate of effective partitioning (1.3 ng/mL/h) could not explain the mineralization rate detected in the absence of biocide (43.9 ng/mL/h). In addition, the C_{eq} value detected (28.3 ng/mL) was significantly lower than the C_{eq} determined in independent, abiotic partitioning experiments with phenanthrene at 1 mg/mL NAPL (50.4 ng/mL − Figure 1A). Similar results were obtained in mineralization experiments with *P. aeruginosa* 19SJ (Figure 3B), in which the levels of endogenously produced rhamnolipids, either in aqueous solution or in suspended cells, remained below the detection limit.

Discussion

The effect of the rhamnolipid biosurfactants above the CMC observed in this study indicates that micellar solubilization is the main mechanism responsible for the enhancement of partitioning of NAPL-dissolved PAH by biosurfactants. Our results agree with other studies reporting the enhanced solubility of pure solid (*11*, *29*) and liquid (*30*) hydrocarbons caused by rhamnolipid biosurfactants. In our study, biosurfactants were more efficient in enhancing partitioning of PAH from HMN than from DEHP, possibly due to their different viscosity and the concomitant difference in diffusion rates of the PAH inside these model NAPLs. The results also show, in a multiple-solute system, that the enhanced partitioning was more evident with more-hydrophobic PAH. A similar observation was made in a study on the effect of the nonionic surfactant Triton X-100 on the solubilization of binary and ternary aqueous mixtures of solid naphthalene, phenanthrene, and pyrene (*31*). That study showed that this differential solubilization can be explained not only on the basis of the individual preference of the more-hydrophobic compounds to be incorporated into the micelle core; in addition, the association of the less-hydrophobic PAH to the interface of the surfactant-micelle core and the bulk water causes a reduction in the core-water interfacial tension, improving the micellar partitioning of more-hydrophobic compounds.

Biosurfactants enhanced the effective partitioning from NAPLs in the presence of model subsurface solids. The effect can be partially attributable to sorbed biosurfactants. At levels below the CMC, they increased the affinity of the solids for aqueous PAH, whereas at levels above the CMC, the K_D values were lower due to competition between micellar and sorbed biosurfactants for PAH partitioning. A previous study (*32*) has shown that sorption of rhamnolipids to soil is an interfacial adsorption process, rather than a process of partitioning into soil organic matter. In the present study, sorbed biosurfactants may have promoted, in turn, sorption of PAH to the solids by modifying their surface hydrophobicity, because of the probable orientation of the hydrophobic moieties of the first biosurfactant layer adsorbed into the aqueous phase. Alternately, PAH may have partitioned into hemimicelles formed by sorbed biosurfactants. Both mechanisms have been previously reported to occur during partitioning of naphthalene and phenanthrene into the synthetic surfactants SDS and Tween 80, sorbed to kaolinite (*33*).

Independently of the strain used, partitioning rates of phenanthrene from HMN in the presence of biodegradation activity were higher than the rate measured in the absence of bacteria. The relatively high final extent of mineralization measured (60%) suggests the complete consumption of the substrate from the NAPL (*12*), being the rest probably converted into biomass and biodegradation products different from CO_2. These observations agree with previous studies with NAPL-associated hydrocarbons, performed in NAPL/water systems designed to create bioavailability restrictions to biodegradation (*16*−*21*). Our results further indicate that, under the experimental conditions used,

biosurfactant production was not the mechanism involved. Instead, the enhancement could be attributed to bacteria growing at the NAPL−water interface. Only when an adhesion-inhibiting agent, Triton X-100, was added to the system did biodegradation-driven partitioning match the abiotic rate. Furthermore, the good agreement showed between those two rates excludes any possible toxic effect of the surfactant on the degrading microbial population. The progressive decrease in mineralization rate observed in the presence of the surfactant can be probably due to depletion of phenanthrene inside the NAPL phase or to the subsequent difficulty of the bacterium to mineralize the compound that was associated to surfactant micelles.

The occurrence of very similar biodegradation rates by bacteria differing in hydrophobicity, adhesion capacity, and, possibly, specific growth rate at the NAPL/water interface suggests that biodegradation was not limited by biological factors. It is conceivable, however, that these physiological traits may cause, in some circumstances, differences in biodegradation rate. For example, recent research has shown that many soil bacteria able to perform growth-linked biodegradation of PAH of three or more rings belong to the genus *Mycobacterium* and seem to be specialized in the degradation of these pollutants by exhibiting strongly adhesive properties and the capacity to form biofilms on solid PAH (*23*, *34*). In addition, a relevant role of cell adhesion and interfacial growth has also been shown for biodegradation of liquid hydrocarbons such as hexadecane (*35*). Adhered cells may enhance the acquisition of their substrates, and therefore the partitioning from the NAPL, by facilitated transfer through cell-associated hydrophobic components or by increasing the concentration gradient near the NAPL−water interface (*20*). Our results extend those findings by further showing that even the most hydrophilic strain (*Sphingomonas* sp. LH128) was able to colonize the NAPL−water interface and to drive partitioning to maximum values.

Diffusion of phenanthrene inside the NAPL was probably the abiotic rate-limiting process acting upon adhered bacteria. The overall resistance to mass transfer of a chemical between two phases is commonly represented as the sum of the individual mass transfer resistances in each phase, which depend on the respective diffusion coefficients and length. The aqueous phase resistance is usually considered the limiting step in the NAPL/water partitioning of hydrophobic compounds, such as PAHs. Nevertheless, for certain situations, for example with highly viscous or semisolid NAPLs, the organic phase resistance can become limiting, after a zone depleted of PAHs develops in the NAPL side (*36*, *37*). In our study, the fact that dissimilar microorganisms were able to enhance the partitioning rate significantly to similar values is in agreement with a scenario in which, in abiotic conditions, the aqueous phase was the limiting step, whereas during biodegradation, a limitation was imposed on the NAPL side. In the case of such limitation, a PAH-depleted zone in the NAPL would have arisen during this period of maximum mineralization. In our study, the significant delay detected in the appearance of phenanthrene in the aqueous phase after stopping biodegradation with a biocide suggests the existence of this depleted zone in the NAPL phase, caused by active biodegradation. Such delay would also have been observed if the biocide required a similar period to be effective, but the immediate inhibition of $^{14}CO_2$ evolution upon addition of the biocide makes this alternative improbable.

It is also possible that the aqueous resistance at the interface was modified by the presence of adhered microbial cells and associated extracellular polymeric substances, formed in the initial stages of phenanthrene biodegradation. This, in addition to the existence of a PAH-depleted zone in the NAPL, may have contributed to the delays observed in formaldehyde experiments. In fact, microbial biofilms may act as hydrophobic, alternative partitioning phases, by decreasing the dissolution of naphthalene crystals into the bulk aqueous phase by up to 90% (*38*) and by significantly sorbing benzene, toluene, and xylene from aqueous solutions (*39*). Given the relevance, shown in this study, of adhered bacteria in the biodegradation of NAPL constituents, and that biofilms are probably present at NAPL−water interfaces exposed for some time to microbial populations from soils and aquifers, the exact contribution of interfacial growth to PAH partitioning and NAPL aging (*40*) should be the subject of further investigation.

The data show that partitioning was increased by biosurfactants in solution at a concentration above the CMC, by biosurfactants sorbed to suspended humic acid−clay colloids, and by active microbial populations degrading the pollutant in situ. Our study suggests therefore that partitioning of PAH may be efficiently enhanced by in situ treatments of NAPL pollution involving the use of biosurfactants and/or biodegradation. The selection of appropriate PAH-degrading strains, able to be transported efficiently through the subsurface and to reach and colonize the NAPL/water surfaces, seems a reasonable step during the design of bioaugmentation strategies for decontamination of soils and aquifers polluted with PAH-containing NAPLs. The combined effect of biosurfactants and microbial activity on PAH degradation should be the subject of further investigation.

Acknowledgments

Support for this research was provided by the European Union (contracts BIO4-CT97-2015 and QLRT-1999-00326) and Spanish CICYT (grants BIO97-1960-CE, BIO2000-1857-CE and REN2001-3523). Lukas Wick is acknowledged for revision of the present work.

Literature Cited

(1) Peters, C. A.; Knightes, C. D.; Brown, D. G. *Environ. Sci. Technol.* **1999**, *33*, 4499−4507.
(2) Mulligan, C. N.; Yong, R. N.; Gibbs, B. F. *Eng. Geol.* **2001**, *60*, 371−380.
(3) Ali, M. A.; Dzombak, D. A.; Roy, S. B. *Water Environ. Res.* **1995**, *67*, 16−24.
(4) McCray, J. E.; Bai, G.; Maier, R. M.; Brusseau, M. L. *J. Contam. Hydrol.* **2001,** *48*, 45−68.
(5) Alexander, M. *Biodegradation and Bioremediation*; Academic Press: San Diego, CA, 1999.
(6) Mulligan, C. N.; Yong, R. N.; Gibbs, B. F.; James, S.; Bennett, H. P. J. *Environ. Sci. Technol.* **1999**, *33*, 3812−3820.
(7) Herman, D. C.; Artiola, J. F.; Miller, R. M. *Environ. Sci. Technol.* **1995**, *29*, 2280−2285.
(8) Harvey, S.; Elashvili, I.; Valdes, J. J.; Kamely, D.; Chakrabarty, A. M. *Bio/technology* **1990**, *8*, 228−230.
(9) García-Junco, M.; De Olmedo, E.; Ortega-Calvo, J. J. *Environ. Microbiol.* **2001**, *3*, 561−569.
(10) Resina-Pelfort, O.; García-Junco, M.; Ortega-Calvo, J. J.; Comas-Riu, J.; Vives-Rego, J. *FEMS Microbiol. Ecol.* **2003**, *43*, 55−61.
(11) Zhang, Y.; Maier, W. J.; Miller, R. M. *Environ. Sci. Technol.* **1997**, *31*, 2211−2217.
(12) Ghoshal, S.; Ramaswami, A.; Luthy, R. G. *Environ. Sci. Technol.* **1996**, *30*, 1282−1291.
(13) Ortega-Calvo, J. J.; Birman, I.; Alexander, M. *Environ. Sci. Technol.* **1995,** *29*, 2222−2225.
(14) Labare, M. P.; Alexander, M. *Environ. Toxicol. Chem.* **1995**, *14*, 257−265.
(15) Fu, M. H.; Alexander, M. *Appl. Microbiol. Biotechnol.* **1995**, *43*, 551−558.
(16) Bouchez, M.; Blanchet, D.; Vandecasteele, J.-P. *Microbiology* **1997**, *143*, 1087−1093.
(17) Efroymson, R. A.; Alexander, M. *Environ. Sci. Technol.* **1994**, *28*, 1172−1179.
(18) Efroymson, R. A.; Alexander, M. *Environ. Sci. Technol.* **1995**, *29*, 515−521.
(19) Carroquino, M. J.; Alexander, M. *Environ. Toxicol. Chem.* **1998**, *17*, 265−270.

(20) Ortega-Calvo, J. J.; Alexander, M. *Appl. Environ. Microbiol.* **1994,** *60*, 2643−2646.
(21) Osswald, P.; Bayeve, P.; Block, J. C. *Biodegradation* **1996**, *7*, 297−302.
(22) Schwarzenbach, R. P.; Gschwend, P. M.; Imboden, D. M. *Environmental Organic Chemistry*; John Wiley & Sons: New York, 1993.
(23) Bastiaens, L.; Springael, D.; Wattiau, P.; Harms, H.; deWatchter, R.; Verachtert, H.; Diels, L. *Appl. Environ. Microbiol.* **2000**, *66*, 1834−1843.
(24) Bendinger, B.; Rijnaarts, H. H. M.; Altendorf, K.; Zehnder, A. J. B. *Appl. Environ. Microbiol.* **1993**, *59*, 3973−3977.
(25) Déziel, E.; Paquette, G.; Villemur, R.; Lépine, F.; Bisaillon, J.-G. *Appl. Environ. Microbiol.* **1996**, *62*, 1908−1912.
(26) Déziel, E.; Lepine, F.; Dennie, D.; Boismenu, D.; Mamer, O. A.; Villemur, R. *Biochim. Biophys. Acta* **1999**, *1440*, 244−252.
(27) Lahlou, M.; Harms, H.; Springael, D.; Ortega-Calvo, J. J. *Environ. Sci. Technol.* **2000,** *34*, 3649−3656.
(28) Lahlou, M.; Ortega-Calvo, J. J. *Environ. Toxicol. Chem.* **1999**, *18*, 2729−2735.
(29) Zhang, Y.; Miller, R. M. *Appl. Environ. Microbiol.* **1992**, *58*, 3276−3282.
(30) Thangamani, S.; Shreve, G. S. *Environ. Sci. Technol.* **1994**, *28*, 1993−2000.
(31) Guha, S.; Jaffé, P. R.; Peters, C. A. *Environ. Sci. Technol.* **1998**, *32*, 930−935.
(32) Noordman, W. H.; Brusseau, M. L.; Janssen, D. B. *Environ. Sci. Technol.* **2000**, *34*, 832−838.
(33) Ko, S.-O.; Schlautman, M. A.; Carraway, E. R. *Environ. Sci. Technol.* **1998**, *32*, 2769−2775.
(34) Wick, L. Y.; Colangelo, T.; Harms, H. *Environ. Sci. Technol.* **2001**, *35*, 354−361.
(35) Rosenberg, M.; Rosenberg, E. *J. Bacteriol.* **1981**, *148*, 51−57.
(36) Ortiz, E.; Kraatz, M.; Luthy, R. G. *Environ. Sci. Technol.* **1999**, *33*, 235−242.
(37) Schluep, M.; Imboden, D.; Gäll, R.; Zeyer, J. *Environ. Toxicol. Chem.* **2001**, *20*, 459−466.
(38) Mulder, H.; Breure, A. M.; Van Honschooten, D.; Grotenhuis, J. T. C.; Van Andel, J. G. *Appl. Microbiol. Biotechnol.* **1998**, *50*, 277−283.
(39) Späth, R.; Flemming, H.-C.; Wuertz, S. *Water Sci. Technol.* **1998**, *37*, 207−210.
(40) Luthy, R. G.; Ramaswami, A.; Ghoshal, S.; Merkel, W. *Environ. Sci. Technol.* **1993**, *30*, 2914−2918.

Received for review September 26, 2002. Revised manuscript received April 7, 2003. Accepted April 29, 2003.

ES020197Q